AIAA 2001-0196

Computational Studies of Magnetic Control in Hypersonic Flow

J. Poggie
D. V. Gaitonde
US Air Force Research Laboratory
Wright-Patterson AFB, OH 45433-7521

39th Aerospace Sciences Meeting & Exhibit
8-11 January 2001 / Reno, NV

For permission to copy or republish, contact the American Institute of Aeronautics and Astronautics 1801 Alexander Bell Drive, Suite 500, Reston, VA 20191–4344

Computational Studies of Magnetic Control in Hypersonic Flow

J. Poggie*
D. V. Gaitonde†
US Air Force Research Laboratory
Wright-Patterson AFB, OH 45433-7521

Computational and theoretical studies of a Mach 5 flow over a hemisphere were carried out to examine the possibility of heat transfer mitigation through magnetic control. Computations employing the low magnetic Reynolds number approximation were compared to a local solution for the stagnation point flow developed by W. B. Bush. Both models indicate that an imposed dipole field can slow the flow in the conductive shock layer and consequently reduce the wall heat flux in the vicinity of the stagnation point. The theoretical model predicts a somewhat higher level of heat transfer than that obtained computationally, but there is good agreement between the two models in the fractional change in heat transfer with increasing strength of the applied magnetic field. For both models, nonuniform electrical conductivity was found to reduce the effectiveness of a given applied field. Magnetic flow control is seen to have a sound physical basis, and may prove to be a useful technology for heat transfer mitigation.

Nomenclature

Roman Symbols

a	= sound speed
$\vec{B}$	= magnetic field
C_p	= constant pressure specific heat
e	= internal energy
$\vec{E}$	= electric field
h	= enthalpy
$\vec{j}$, $\vec{J}$	= electric current
k	= thermal conductivity
p	= pressure
q	= charge density
$\vec{Q}$	= heat flux
r, θ, ϕ	= spherical coordinates
R	= radius
t	= time
T	= temperature
u, v, w	= Cartesian velocity components
$\vec{v}$, V	= fluid velocity
x,y,z	= Cartesian coordinates

Greek Symbols

γ	= specific heat ratio
Δ	= shock standoff
ϵ_0	= permittivity of vacuum
η	= magnetic diffusivity, $1/\sigma\mu_0$
λ	= second viscosity coefficient
μ	= dynamic viscosity
μ_0	= permeability of vacuum
ρ	= density
σ	= electrical conductivity
Σ	= stress tensor
$\vec{\omega}$	= vorticity

Subscripts

0	= reference value
b	= body
e	= boundary layer edge
g	= imposed conditions
m	= magnetic
s	= shock
w	= wall
∞	= freestream

*Research Aerospace Engineer, Air Vehicles Directorate, AFRL/VAAC, 2210 Eighth Street. Senior Member AIAA.
†Research Aerospace Engineer, Air Vehicles Directorate, AFRL/VAAC, 2210 Eighth Street. Associate Fellow AIAA.
This paper is a work of the U.S. Government and is not subject to copyright protection in the United States.

Introduction

THE extremely high temperatures in the shock layer at the blunt nose of a hypersonic vehicle remain one of the prime impediments to routine trans-atmospheric flight. Given the ionization associated with these high temperatures, it is natural to consider electromagnetic control of this class of flows. Since the Lorentz force tends to oppose fluid motion across magnetic field lines, a magnetic field applied to the conductive shock layer would tend to increase the drag of a vehicle (a desirable effect for atmospheric entry), and, by slowing the flow near the surface of the body, reduce heat transfer and skin friction.

The origin of this idea dates to the mid 1950s.[1–5] Various system concepts envisioned both local flow control for stagnation point heat transfer reduction and large-scale, self-powered magnetogasdynamic sys-

tems[3,6,7] which would increase the drag of a vehicle, reducing the overall heat load during atmospheric entry.[8] Vehicle control through asymmetric forces[6,9] or the Hall effect[7] was also proposed, as was a combination of ablative and magnetic heat transfer mitigation.[10]

Enthusiasm for the practical application of these ideas waned by the early 1960s, and publication on the subject tapered off after that decade. In a comprehensive review of the literature on electromagnetic control of heat transfer, Romig wrote: "Eventually ... it was concluded that the field strengths necessary to provide sufficient shielding against high-heat fluxes during atmospheric flight were not competitive (in terms of weight) with other methods of cooling" (Ref. 11, p. 269). Particular problems included increased radiative heat transfer under magnetic control, Joule heating in the electromagnet, and the extremely strong magnetic fields needed for the low conductivity levels of thermally-ionized air. Many authors, however, held out the possibility that artificial ionization and superconducting magnets could change the situation to the point where electromagnetic control could become practical.[11] Considerable improvement in these technologies has occurred in the forty-five years since the first suggestion of electro-magnetic control for hypersonic flight, and it is now appropriate to reconsider this technique.

Magnetogasdynamic Blunt Body Flow

The first analytical models for this problem involved similarity solutions for a stagnation point flow.[12–16] A uniform magnetic field, unaffected by the flow, was taken to be oriented normal to the wall. A model for the inviscid outer flow was considered in which the pressure gradient was fixed and the magnetic force set the velocity gradient. Compressibility effects in the shock layer were neglected. Shear stress and heat flux at the wall were found to be strongly reduced as the imposed field strength was increased, primarily due to the decreased streamwise velocity gradient at the boundary layer edge.[15]

Later studies[17–22] improved the model of the inviscid outer flow by modifying the constant density theory developed for non-magnetic blunt body flow.[23] The imposed magnetic field was taken to be an axisymmetric dipole, a fairly realistic model for the field generated by an electromagnet. These models eliminated the fixed pressure gradient approximation used in the earlier studies, and also predicted an increase in shock standoff.

The improved inviscid-flow models were matched to similarity solutions[24–26] for the stagnation point boundary layer which avoided the constant property assumption of earlier studies. The combined model again predicted a significant reduction in stagnation point heat transfer. An interesting result of the variable property boundary layer calculations[26] was that, under certain conditions, variable electrical conductivity could reduce the effectiveness of control and produce overshoot boundary layer profiles. This effect is a result of the diminished magnitude of the magnetic force due to reduced electrical conductivity near a cold wall.[27]

Early numerical studies attempted to address some of the approximations in the analytical inviscid-flow models.[28–30] The computations showed the same trends as the analytical studies: increased shock standoff and reduced stagnation point velocity gradient. Computations using more recent methods[31,32] seem to confirm these trends.

Experiments have at least qualitatively confirmed the theoretical predictions. Shock standoff, inferred from photographs of the glowing shock-layer plasma in wind tunnel tests, has been found to increase with applied field strength.[17,33–36] A reduction in heat transfer rate[37] and an increase in drag[34–36] have also been observed experimentally.

A number of complicating effects have been examined in theoretical studies. Magnetic control was studied in the low Reynolds number, merged shock layer regime using thin shock layer theory,[35,38–44] and it was found that the effect of magnetic control may be reduced for very low Reynolds numbers. The Hall current, which becomes significant under high altitude, low density conditions, also tends to reduce the effectiveness of control.[45,46] Similarly, the induced magnetic field tends to oppose the applied magnetic field and diminish control effectiveness when the magnetic Reynolds number is relatively high.[18,46,47]

In the present study, we have considered the problem of a Mach 5, ideal gas flow over a hemisphere, which was addressed in the early inviscid computations of Coakley and Porter.[31] Both inviscid and viscous computations were carried out using a low magnetic Reynolds number model, and the results were compared to the theory developed by Bush[18,26] as well as the Coakley-Porter computations. In particular, we have examined magnetic control of the heat transfer in the vicinity of the stagnation point, and the influence of conductivity variation on the efficacy of this technique.

Physical Model

A very general continuum model for a flow affected by electromagnetic forces would include the full set of Maxwell's equations coupled to the fluid conservation equations. The conservation equations of mass, momentum, and energy are expressed as:

$$\frac{\partial \rho}{\partial t} + \nabla \cdot (\rho \vec{v}) = 0 \quad (1)$$

$$\frac{\partial}{\partial t}(\rho \vec{v}) + \nabla \cdot (\rho \vec{v}\vec{v} - \mathbf{\Sigma}) = \vec{f} \quad (2)$$

$$\frac{\partial}{\partial t}(\rho E_t) + \nabla \cdot (\rho \vec{v} E_t - \mathbf{\Sigma} \cdot \vec{v} + \vec{Q}) = P \quad (3)$$

where $E_t = e + v^2/2$, $\vec{f}$ is the electromagnetic body force, and P is a power source term. Maxwell's equations can be expressed as follows using SI units:

$$\epsilon_0 \nabla \cdot \vec{E} = q \quad (4)$$

$$\nabla \cdot \vec{B} = 0 \quad (5)$$

$$\nabla \times \vec{E} = -\frac{\partial \vec{B}}{\partial t} \quad (6)$$

$$\nabla \times \vec{B}/\mu_0 = \vec{j} + \epsilon_0 \frac{\partial \vec{E}}{\partial t} \quad (7)$$

These are Gauss's law, conservation of magnetic flux, Faraday's law, and the Ampère-Maxwell law, respectively. The charge conservation equation

$$\frac{\partial q}{\partial t} + \nabla \cdot \vec{j} = 0 \quad (8)$$

can be derived from these equations. Neglecting magnetization and polarization of the fluid, the total current is the sum of the convected charge and the conduction current: $\vec{j} = q\vec{v} + \vec{J}$, the force per unit volume of matter (Lorentz force) is $\vec{f} = q\vec{E} + \vec{j} \times \vec{B}$, and the power delivered to matter by the field is $P = \vec{E} \cdot \vec{j}$.

In the case where typical flow length scales are much larger than the Debye length, flow time scales are larger than the reciprocal of the plasma frequency, and flow velocities are much less than the speed of light, a simplified magnetogasdynamic (MGD) model is applicable. The displacement current $\epsilon_0 \partial \vec{E}/\partial t$ and the convected charge $q\vec{v}$ are neglected as small compared to the conduction current $\vec{J}$. Since charge separation is small, the force due to the electric field and the unsteady term in Eq. (8) are also neglected. Maxwell's equations can be reduced to:

$$\nabla \cdot \vec{J} = 0 \quad (9)$$

$$\nabla \cdot \vec{B} = 0 \quad (10)$$

$$\nabla \times \vec{E} = -\partial \vec{B}/\partial t \quad (11)$$

$$\nabla \times \vec{B}/\mu_0 = \vec{J} \quad (12)$$

The force on the fluid is $\vec{f} = \vec{J} \times \vec{B}$ and the power delivered to the fluid is $P = \vec{E} \cdot \vec{J}$.

For simplicity, we assume in the present work that the current is given by Ohm's law:

$$\vec{J} = \sigma(\vec{E} + \vec{v} \times \vec{B}) \quad (13)$$

A scalar electrical conductivity is a good approximation if the collision frequency is much greater than the cyclotron (gyro) frequency, as in a relatively dense gas. Equations (9)-(13) can be combined to eliminate the electric field, giving the magnetic induction equation:

$$\frac{\partial \vec{B}}{\partial t} = \nabla \times \left(\vec{v} \times \vec{B} - \eta \nabla \times \vec{B} \right) \quad (14)$$

This level of model is the starting point for the theory that will be described later.

An order of magnitude analysis of the terms in Eq. (14) reveals that the ratio of the magnitudes of the convective and diffusive terms is given by the magnetic Reynolds number $\mathrm{Re}_m = \sigma \mu_0 V L$. This quantity is small in many aerospace applications. For example, consider a blunt body of 1 m nose radius, flying at 8 km/s at an altitude of 61 km. Assuming chemical equilibrium downstream of the bow shock, the electrical conductivity is about 300 $(\Omega \cdot \mathrm{m})^{-1}$ and the magnetic Reynolds number is $\sigma \mu_0 V_\infty R_b \approx 3$.

For small magnetic Reynolds numbers, the distortion of the magnetic field by the flow can be neglected, and only the imposed field has a significant influence on the flow. The source terms in the conservation equations are given by:

$$\vec{f} = \sigma(\vec{E} + \vec{U} \times \vec{B}) \times \vec{B} \quad (15)$$

$$P = \sigma(\vec{E} + \vec{U} \times \vec{B}) \cdot \vec{E} \quad (16)$$

where the electric and magnetic fields are considered known.

For the numerical calculations presented here, we adopted the low magnetic Reynolds number model for the magnetic field. Coupling this model, (15)-(16), with the conservation equations, (1)-(3), a complete set of governing equations for the flow is obtained. The usual constitutive equations for the stress and heat flux in a Newtonian fluid were employed:

$$\Sigma_{ij} = -p\delta_{ij} + \mu \left(\frac{\partial u_i}{\partial x_j} + \frac{\partial u_j}{\partial x_i} \right) + \lambda \frac{\partial u_k}{\partial x_k} \delta_{ij} \quad (17)$$

$$Q_i = -k \frac{\partial T}{\partial x_i} \quad (18)$$

Viscosity was computed using the Sutherland formula for air, and Stokes' hypothesis was adopted: $\lambda = -2\mu/3$. The Prandtl number was taken as constant.

An ideal gas with constant specific heats was assumed as a simple thermodynamic model to illustrate the basic flow physics without the additional complexity of chemically-reacting air. The corresponding equations of state are:

$$T = \frac{p}{R\rho} \quad (19)$$

$$e = \frac{p}{(\gamma - 1)\rho} \quad (20)$$

Electrical conductivity was assumed to be a function of temperature alone.

Numerical Formulation

For the numerical computations, the governing equations (1)-(3) were cast in nondimensional form. The equations were nondimensionalized by the reference quantities ρ_r, V_r, L_r, B_r, μ_0, μ_r, T_r, and σ_r. The

nondimensional variables are then:

$$\begin{array}{lll} t^* = tV_r/L_r & \rho^* = \rho/\rho_r & \vec{v}^* = \vec{v}/V_r \\ \vec{B}^* = \vec{B}/B_r & p^* = p/(\rho_r V_r^2) & e^* = e/V_r^2 \\ \mu^* = \mu/\mu_r & \sigma^* = \sigma/\sigma_r & T^* = T/T_r \end{array} \quad (21)$$

In the present work, the reference values for the magnetic field and the electrical conductivity were taken to be those at the stagnation point. The reference length scale was the body radius, and the other reference values corresponded to the freestream conditions. In the subsequent discussion of the computations, the superscript (*) will be dropped and all quantities will be assumed to be nondimensional unless explicitly stated otherwise.

The overall form of Eqs. (1)-(3) is unchanged by nondimensionalization. The magnetic source terms become:

$$\vec{f} = Q\sigma(\vec{E} + \vec{U} \times \vec{B}) \times \vec{B} \quad (22)$$

$$P = Q\sigma(\vec{E} + \vec{U} \times \vec{B}) \cdot \vec{E} \quad (23)$$

where $Q = \sigma_r B_r^2 L_r/(\rho_r V_r)$ is the magnetic interaction parameter. The nondimensional flux terms become:

$$\Sigma_{ij} = -p\delta_{ij} + \frac{1}{\mathrm{Re}}\left[\mu\left(\frac{\partial u_i}{\partial x_j} + \frac{\partial u_j}{\partial x_i}\right) + \lambda\frac{\partial u_k}{\partial x_k}\delta_{ij}\right] \quad (24)$$

$$Q_i = -\frac{1}{\mathrm{Pr\,Ec\,Re}}\, k\frac{\partial T}{\partial x_i} \quad (25)$$

where $\mathrm{Pr} = \mu C_p/k$ is the Prandtl number, $\mathrm{Ec} = V_r^2/(C_p T_r)$ is the Eckert number, and $\mathrm{Re} = \rho_r V_r L_r/\mu_r$ is the Reynolds number. For the present computations, we assumed that the electric field was zero, and that the magnetic field was an axisymmetric dipole with its origin at the center of the hemispherical body.

The governing equations were solved by first writing the flux-vector form of the governing equations in general curvilinear (ξ, η, ζ) coordinates.[48,49] Each derivative in transformed space $(\Delta\xi = \Delta\eta = \Delta\zeta = 1)$ was approximated with a standard second-order centered formula, *e.g.*:

$$\frac{\partial \phi}{\partial \xi} = \frac{\phi_{i+1} - \phi_{i-1}}{2} \quad (26)$$

A popular second- and fourth-order blend of damping[50] was used to enforce stability. Evolution of the governing equations in time was carried out using the classical four-stage Runge-Kutta method.[51]

Standard boundary conditions on the velocity and temperature, appropriate for the inviscid flow and viscous flow calculations, were used. Axial symmetry was imposed on a three-dimensional grid by using a small number of points (5) in the symmetry direction, and enforcing symmetry at the end of each time step.

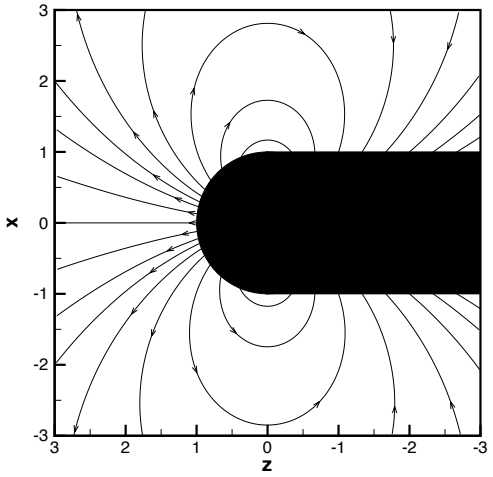

Fig. 1 Schematic diagram of blunt body with imposed magnetic field.

Theoretical Model

Here we describe a local solution[18,26] for the vicinity of the nose of an axisymmetric blunt body in steady hypersonic flow. We assume that the Reynolds number is high enough that the flow can be divided into an inviscid outer flow and a viscous boundary layer. We take the imposed magnetic field to be a dipole located at the center of the sphere, and solve for the induced field. Figure 1 is a schematic diagram of the configuration. The coordinate system is such that $x = r\cos\phi\sin\theta$, $y = r\sin\phi\sin\theta$, and $z = r\cos\theta$, where the z-axis is directed opposite the freestream flow.

Inviscid Flow

The model[18] of the inviscid outer flow uses a modification of the constant density theory originally applied to non-magnetic, hypersonic flows.[23] The solution assumes that both the body and its corresponding bow shock have a spherical shape in the vicinity of the centerline. We also assume that the density and electrical conductivity are constant within the shock layer, and that the freestream electrical conductivity is zero. As a consequence of the assumption of steady flow and axial symmetry, the electric current must flow only in the azimuthal (ϕ) direction, and the electric field must be zero.

The equations are cast in nondimensional form using the freestream velocity V_∞, the shock radius R_s, and the centerline magnetic field strength at the shock B_{s0}. With no electric field, Maxwell's equations reduce to:

$$\nabla \cdot \vec{B} = 0 \quad (27)$$

$$\nabla \times \vec{B} = \mathrm{Re}_{m,s}\, \vec{v} \times \vec{B} \quad (28)$$

For the constant density flow in the shock layer, the continuity equation and the vorticity transport equa-

tion (curl of the momentum equation) become:

$$\nabla \cdot \vec{v} = 0 \quad (29)$$

$$\nabla \times (\vec{\omega} \times \vec{v}) = \frac{Q_s}{K} \nabla \times [(\vec{v} \times \vec{B}) \times \vec{B}] \quad (30)$$

where the only non-zero component of vorticity is in the ϕ-direction: $\vec{\omega} = \omega \hat{e}_\phi$.

Several nondimensional parameters appear in these equations: the interaction parameter $Q_s = \sigma B_{s0}^2 R_s/(\rho_\infty V_\infty)$, the shock density ratio $K = \rho/\rho_\infty$, and the magnetic Reynolds number $\mathrm{Re}_{m,s} = \sigma \mu_0 R_s V_\infty$. We will also use analogous parameters that only depend on information known before solving the problem: $Q = \sigma B_{g0}^2 R_b/(\rho_\infty V_\infty)$ and $\mathrm{Re}_m = \sigma \mu_0 R_b V_\infty$. Here B_{g0} is the field intensity at the nose of the body in the absence of flow.

The magnetic fields just downstream of the shock ($r = 1$) and at the body surface ($r = r_b$) provide boundary conditions for the induction equation (see Ref. 47 for details). For the present work, we assume that the freestream and the body consist of non-conducting and non-magnetic material. We require that the magnetic field approach zero far away from the body, so the nondimensional freestream field becomes:

$$\vec{B} = \frac{\cos\theta}{r^3}\,\hat{e}_r + \frac{\sin\theta}{2r^3}\,\hat{e}_\theta \quad (31)$$

Similarly, the nondimensional field inside the body has the form:

$$\vec{B} = \left(\frac{B_{g0}}{B_{s0}}\frac{r_b^3}{r^3} + C\right)\cos\theta\,\hat{e}_r + \left(\frac{B_{g0}}{B_{s0}}\frac{r_b^3}{2r^3} - C\right)\sin\theta\,\hat{e}_\theta \quad (32)$$

where C is a constant related to the distortion of the imposed dipole field by the flow.

Another set of boundary conditions is provided by the velocity and vorticity just downstream of the shock. In the limit of small conductivity considered here, the magnetic field does not have a direct effect on the shock jump conditions. (It does, however, in the infinite conductivity limit.[52]) Using mass conservation across the shock, we find that the nondimensional radial velocity component is $v_r(1,\theta) = -\cos\theta/K$. The tangential velocity is continuous across the shock, so $v_\theta(1,\theta) = \sin\theta$. The vorticity just downstream of the shock is a function of the shock curvature, the density ratio, and the tangential component of the Lorentz force.[39] In nondimensional terms, the vorticity just downstream of the shock can be expressed as:

$$\omega_\phi = \frac{(K-1)^2}{K}\sin\theta + Q_s\left(1 + \frac{1}{2K}\right)\sin\theta\cos\theta \quad (33)$$

The problem is solved in an inverse manner, specifying the conditions at the shock, and solving for the location of the corresponding body. We write Eqs. (27)-(30) in spherical coordinates, impose inflow boundary conditions at the downstream side of the shock, and march the solution downstream until inviscid wall conditions are satisfied, indicating the location of the body surface. Once the solution has been determined for a given magnetic field at the shock (B_{s0}), we can calculate the net magnetic field strength at the nose of the body ($B_{b0} = B_{s0}|\vec{B}(r_b, 0)|$) and the corresponding imposed field strength (B_{g0}).

Introducing a magnetic potential of the form $M(r)\sin^2\theta$ and an analogous stream function of the form $F(r)\sin^2\theta$, we find magnetic and velocity fields that satisfy Eqs. (27) and (29) and are consistent with the boundary conditions at the shock. Substituting these forms into Eqs. (28) and (30), we find that a θ-dependence remains, unless we use the small angle approximations $\sin\theta \approx \theta$ and $\cos\theta \approx 1$ for the trigonometric functions. Under these conditions, a self-similar form is obtained, and the vorticity transport and induction equations reduce to ordinary differential equations. (See Ref. 18 for the full equations.)

In the example calculations that will be presented later, these ordinary differential equations were integrated using an adaptive Runge-Kutta-Fehlberg 4-5 method, from the initial conditions at the shock until vanishing normal velocity was obtained at the body surface. Calculations were carried out for a fixed Q and Re_m; iteration was used to find the corresponding values of Q_s and $\mathrm{Re}_{m,s}$.

Limitations

The constant density theory is based on the assumption that, for a strong bow shock, the flow in the vicinity of the nose of a blunt body is effectively incompressible, since the Mach number in that region is very low. A local solution is developed for the vicinity of the stagnation point, assuming constant density in that region.

The major drawback of the constant density approach is that the density ratio varies along the bow shock in a real blunt body flow, so that the flow is more realistically modeled as a stratified, rather than constant density, flow ($D\rho/Dt = 0$, rather than $\rho = \text{const}$). Nevertheless, constant density theory gives a reasonable estimate of the shock standoff distance for large shock density ratios at the nose.

Figure 2, for example, compares theoretical predictions[23] to an experimental correlation[53] for shock standoff in non-magnetic air flow over a sphere. The prediction tends to be a bit low, but improves as the shock density ratio is increased. For density ratios of $K \geq 3$, the predicted standoff is within 15% of the experimental data.

Viscous Boundary Layer

We examine the flow near the wall using laminar boundary layer theory.[26] If we assume that there

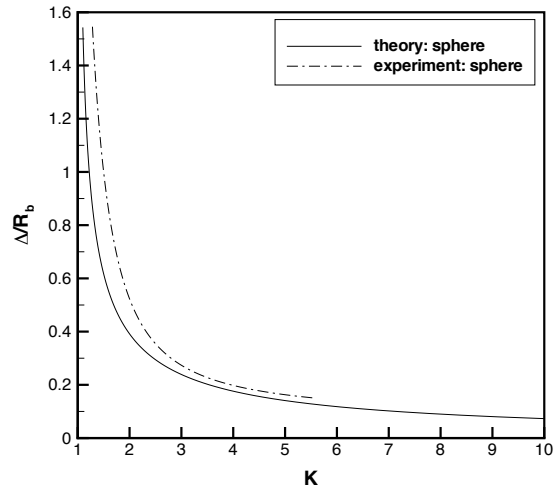

Fig. 2 Standoff distance versus shock density ratio for sphere: non-magnetic constant density theory and experiment.

are no electrodes to introduce a potential difference, then it is valid to take the electric field as zero in steady flow. We assume that current only flows in the transverse direction, and that there is no fluid flow in that direction. Making the usual assumptions of boundary layer theory, we can show that only the wall-normal component of the magnetic field has a significant influence on the boundary layer flow. We use an orthogonal, curvilinear coordinate system (x, y, z) with the origin at the stagnation point, and $y = 0$ on the body surface.

In the MGD boundary layer approximation, the equation for conservation of mass is:

$$\frac{\partial}{\partial x}\left(\rho u r^m\right) + \frac{\partial}{\partial y}\left(\rho v r^m\right) = 0 \tag{34}$$

where $r(x)$ is the body radius, and $m = 0$ for planar symmetry and $m = 1$ for axial symmetry. The conservation of momentum is expressed as:

$$\rho u\frac{\partial u}{\partial x} + \rho v\frac{\partial u}{\partial y} = -\frac{dp}{dx} + \frac{\partial}{\partial y}\left(\mu\frac{\partial u}{\partial y}\right) - \sigma B_y^2 u \tag{35}$$

where $B_y = B_y(x)$. In the freestream, the momentum equation reduces to:

$$\frac{dp}{dx} = -\left(\rho_e u_e\frac{du_e}{dx} + \sigma_e B_y^2 u_e\right) \tag{36}$$

The equation for the conservation of energy has the form:

$$\rho u\frac{\partial h}{\partial x} + \rho v\frac{\partial h}{\partial y} = u\frac{dp}{dx} + \frac{\partial}{\partial y}\left(k\frac{\partial T}{\partial y}\right) + \mu\left(\frac{\partial u}{\partial y}\right)^2 + \sigma B_y^2 u^2 \tag{37}$$

The boundary conditions at the wall are no slip and no temperature jump. At the boundary layer edge, the solution must match the inviscid outer flow.

For an axisymmetric stagnation point boundary layer, $m = 1$, $r = x$, and $u_e = Gx$, where $G = (du_e/dx)_0$ is constant. For a uniform magnetic field $(B_y = B_{b0})$, a similarity solution can be obtained with the introduction of new independent variables

$$\xi(x) = \frac{1}{2(m+1)}\rho_e\mu_e G x^{2(m+1)} \tag{38}$$

$$\eta(x,y) = \sqrt{\frac{(m+1)G}{\rho_e\mu_e}}\int_0^y \rho d\hat{y} \tag{39}$$

and dependent variables $u = u_e(\xi)f'(\eta)$ and $h = h_e(\xi)g(\eta)$. The resulting set of ordinary differential equations is given in Ref. 26.

Example boundary layer calculations were carried out for the edge conditions predicted by constant density theory. The adaptive Runge-Kutta-Fehlberg 4-5 method was again used to numerically integrate the ordinary differential equations of the similarity solution. The boundary conditions were satisfied by a shooting scheme based on Newton-Raphson iteration.

Results

The case of a Mach 5, ideal gas flow over a hemisphere was chosen to match the inviscid computations of Coakley and Porter.[31] The results were compared to these early computations and to the inviscid theory of Bush[18] (with $\mathrm{Re}_m = 0$). Additional viscous calculations were carried out to examine the influence of magnetic control on the heat transfer in the vicinity of the stagnation point. To allow comparison with Bush's boundary layer theory,[26] a relatively high Reynolds number, $\rho_\infty V_\infty R_b/\mu_\infty = 80000$, was chosen, with an assumption of laminar flow. The corresponding dimensional conditions are a body of 10 mm radius and a freestream temperature of 100 K.

Inviscid Flow

The conditions for the baseline inviscid flow case were $M = 5$ and $\gamma = 1.4$, with a corresponding shock density ratio of $K = 5$. (Here $M = V_\infty/a_\infty$ is the Mach number.) The inviscid computations were carried out on a grid of $60 \times 40 \times 5$ points distributed, respectively, in the directions along the body surface, normal to the body, and in the circumferential direction.

The basic flow structure is illustrated in Fig. 3, which shows the pressure field predicted by the numerical computations for two cases: $Q = 0$ and $Q = 6$. (Note that the coordinate system is different from that in Fig. 1.) With the application of a strong magnetic field, there is a dramatic increase in the shock standoff, but little qualitative change in the flow structure.

The increase in shock standoff with interaction parameter is quantified in Fig. 4. The predictions

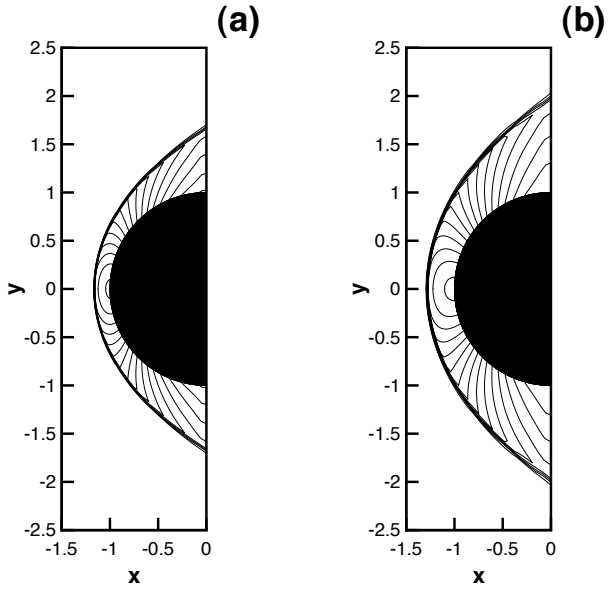

Fig. 3 Pressure field p/p_∞ for inviscid flow (contour interval 2). (a) $Q = 0$ (b) $Q = 6$

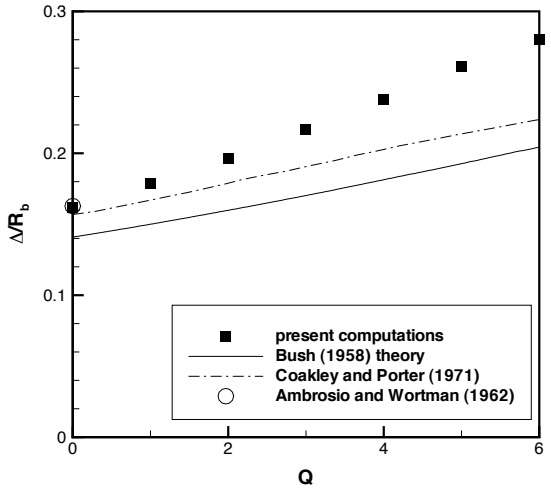

Fig. 4 Effect of applied magnetic field on shock standoff ($M = 5$, $\gamma = 1.4$).

of Bush's theory,[18] Coakley and Porter's computations,[31] and the correlation of Ambrosio and Wortman[53] are shown for comparison with the results of the present computations. The computed standoff increases from a value of $\Delta/R_b = 0.163$, consistent with the empirical correlation for the non-magnetic case, to a value of 0.280 at $Q = 6$.

As expected for a constant-density calculation, the prediction of the Bush theory tends to be too low for the non-magnetic case (about 14% below the empirical value), whereas the results from Coakley and Porter and the present computations are close to the empirical correlation. Although all methods predict higher standoff with increasing interaction parameter,

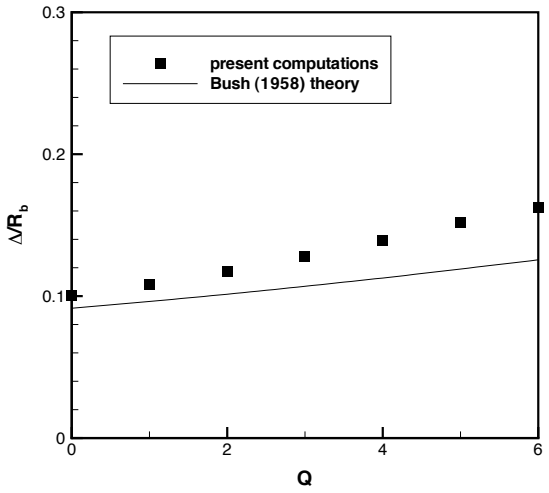

Fig. 5 Effect of applied magnetic field on shock standoff ($M = 5$, $\gamma = 1.2$).

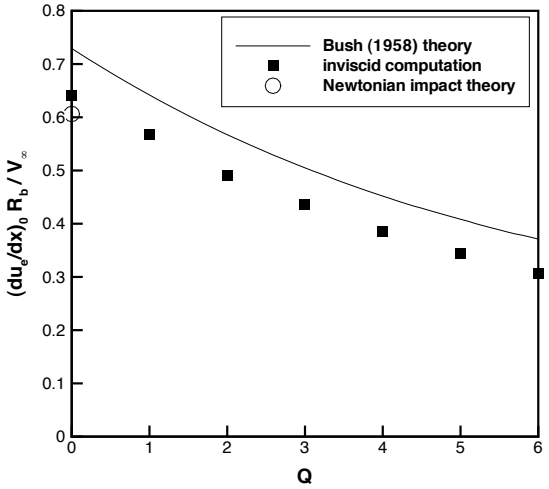

Fig. 6 Effect of applied magnetic field on surface velocity gradient ($M = 5$, $\gamma = 1.4$).

the present computations show a more rapid rise.

Noting that the predictions of constant-density theory should become more accurate with increasing shock strength, we investigate this phenomenon further by examining a stronger shock case, as shown in Fig. 5. For this case the Mach number is held fixed at $M = 5$, but the adiabatic exponent is reduced to $\gamma = 1.2$, giving a shock density ratio of $K \approx 7.9$. Here the prediction of Bush's theory and the prediction of the numerical computations are significantly closer. These results suggest that the primary source of the discrepancy between the computational and theoretical results is associated with the constant density assumption in the theoretical approach.

Since the magnetic force tends to oppose flow across the magnetic field lines, the effect of the applied field

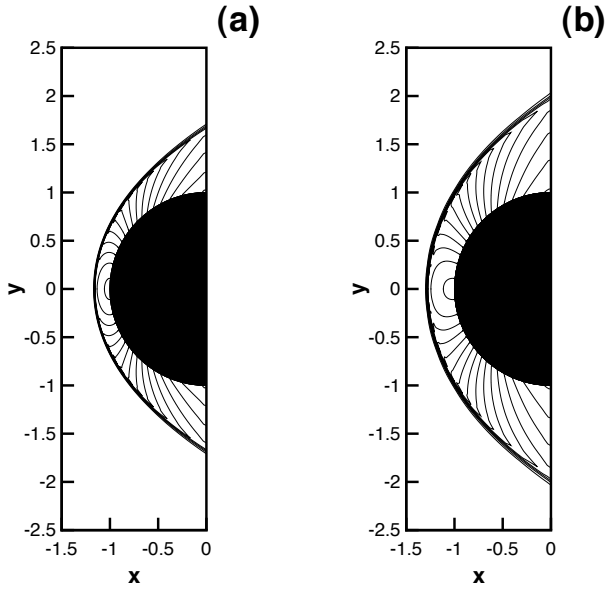

Fig. 7 Pressure contours p/p_∞ for viscous computations (fine grid, contour interval 2). (a) $Q = 0$. (b) $Q = 6$.

is to slow the flow. This effect is illustrated in Fig. 6, which shows a significant reduction in the stagnation point velocity gradient with increasing field strength. The solid line indicates the prediction of Bush's theory, and the filled symbols indicate results derived from the inviscid-flow computations. For reference, the open symbol locates the prediction of Newtonian impact theory. The computational results are seen to fall somewhat below the values predicted by the Bush theory, but there is excellent agreement in the trend with increasing interaction parameter. For the non-magnetic case, the Newtonian impact theory predicts a velocity gradient slightly below that derived from the corresponding computations.

Viscous Flow

A corresponding set of viscous computations was carried out for Mach 5 flow with $\gamma = 1.4$ and Re $=$ 80000. Two grids were used: a baseline case with $60 \times 80 \times 5$ points, and a finer grid of $120 \times 160 \times 5$ points. For these calculations electrical conductivity was taken to be constant through the boundary layer – the issue of variable conductivity will be considered in the next section.

Although some theoretical studies have shown a decrease in effectiveness of magnetic control under conditions where viscous effects are very strong,[35,38,44] the overall flow structure is essentially unchanged by viscous effects in the present high Reynolds number case. Figure 7 shows the pressure contours for the viscous computations on the fine grid. The viscous-flow pressure field is seen to be very similar to that shown previously in Fig. 3 for the inviscid case, and again the shock standoff distance increases significantly with an

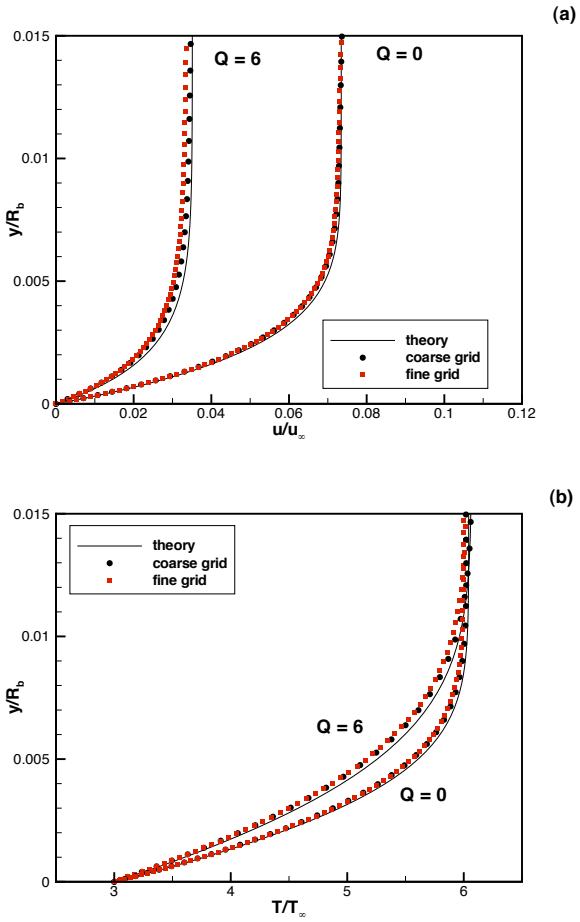

Fig. 8 Boundary layer profiles, $\theta = 6.6°$.

applied magnetic field.

Figure 8 shows boundary layer profiles of velocity and temperature for a station close to the centerline ($\theta = 6.6°$). (Here, following the usual boundary layer notation, y is the wall-normal coordinate.) The circular and square symbols show, respectively, the results from the coarse and fine grid computations. The solid lines indicate the predictions of Bush's similarity solution.[26] Since the inviscid theory tends to underestimate the velocity gradient at the boundary layer edge (see Fig. 6), the edge conditions from the inviscid computation were used as input for the similarity solution. Excellent overall agreement is obtained between theory and computation, and it is evident that results of the computations are practically mesh-independent.

Both computation and theory reproduce the 'full' velocity profile expected for the non-magnetic stagnation point boundary layer ($Q = 0$ case in Fig. 8a). With the application of a strong magnetic field ($Q = 6$ case in Fig. 8a), the magnetic force effectively counteracts the favorable pressure gradient, decelerating the freestream and strongly reducing the velocity gradient $\partial u/\partial y$ at the wall. A similar trend is seen with the temperature profiles (Fig. 8b). The applied magnetic field causes a reduction in the temperature gradient

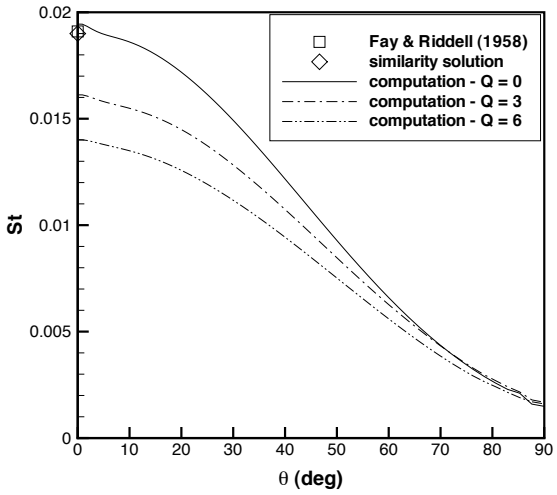

Fig. 9 Effect of applied magnetic field on surface heat transfer profile.

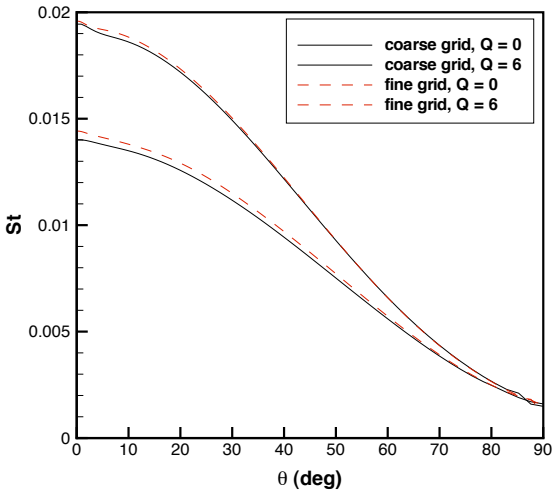

Fig. 10 Effect of grid resolution on computed surface heat transfer profile.

$\partial T/\partial y$ at the wall, with a corresponding reduction in the wall heat flux.

Figure 9 shows the computed Stanton number ($\mathrm{St} = q_w/[\rho_\infty u_\infty C_p(T_w - T_\infty)]$) profile around the body surface. The lines indicate the computational results (coarse-grid) for different values of the interaction parameter, whereas the symbols indicate the stagnation point value computed using the Fay-Riddell[54] correlation and using a similarity solution of the non-magnetic boundary layer equations. For the latter two calculations, the boundary layer edge velocity gradient is taken to be the value predicted by Newtonian impact theory (see Ref. 55, pp. 596-600).

The heat transfer profile in the non-magnetic case ($Q = 0$) is typical of that seen for hypersonic flow over spheres and cylinders (see Ref. 56, p. 258). As θ is reduced, the computed profile approaches closely the values predicted by the correlation and similarity solution.

An applied magnetic field is seen, in the computations, to reduce the level of heat transfer over the major portion of the hemisphere, with the greatest reductions in the vicinity of the stagnation point. The heat transfer does not change near $\theta = 90°$ because the velocity vector and magnetic field vector are nearly collinear in this part of the flow.

A small bump is detectable in the portion of the computed profile near $\theta = 0°$: this is a numerical artifact produced by the finite difference method near the Jacobian singularity at the axis of symmetry. This issue is examined in more detail in Fig. 10, which compares the Stanton number profiles obtained for the coarse and fine grid computations. The close agreement of the two sets of computations indicates that adequate computational resolution is achieved with the coarse grid solution, and it is seen that the centerline anomaly diminishes with mesh refinement.

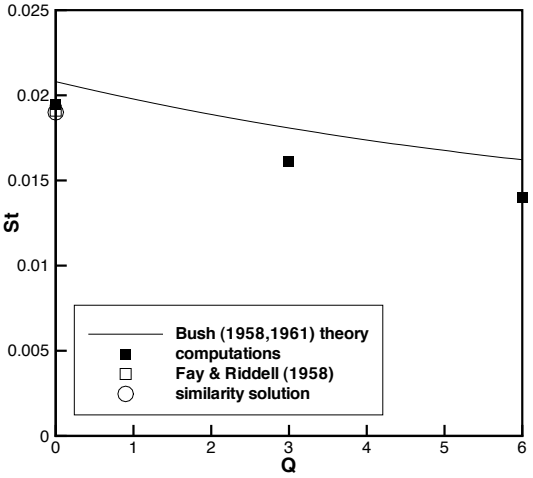

Fig. 11 Effect of applied magnetic field on stagnation point heat transfer.

Figure 11 shows the Stanton number at the stagnation point as a function of the interaction parameter. The solid line represents the predictions of the combined constant density and boundary layer theories of Bush, the filled symbols are the results of the coarse-grid computations, and the open symbols represent the Fay-Riddell correlation and corresponding similarity solution. In the non-magnetic case, the computations are in good agreement with the latter heat transfer theories, whereas the prediction of Bush's theory is somewhat higher. Both theory and numerical computation predict a significant decrease in the heat transfer rate with increasing strength of the applied field, and there is good agreement between the two models in the fractional change in heat transfer. Again, the overall

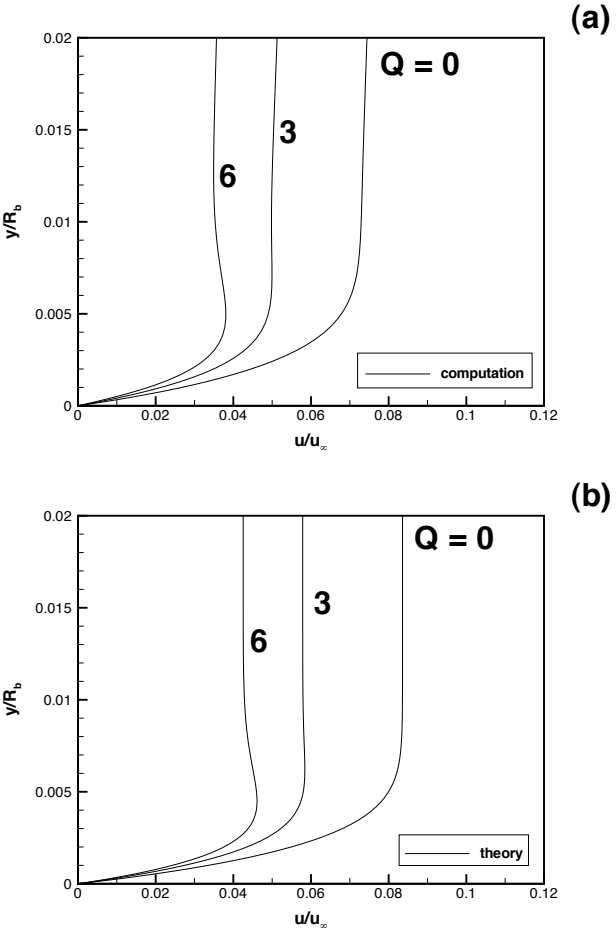

Fig. 12 Effect of variable conductivity on boundary layer velocity profiles at $\theta = 6.6°$. (a) Computational results (coarse grid). (b) Predictions of combined constant-density theory and boundary layer theory.

higher value predicted by Bush's theory is probably due to an overestimate of du_e/dx (see Fig. 6).

Variable Conductivity

The variable-property boundary layer calculations of Bush[26] showed that variable electrical conductivity tended to reduce the effectiveness of control, and to produce overshoot velocity profiles under certain conditions. Bush showed, using an asymptotic expansion, that overshoot profiles occur for a cold-wall boundary layer when $\sigma_e B_{b0}^2/(\rho_e\ du_e/dx) > 1/n$ if the conductivity is given by $\sigma \propto T^n$. The physical mechanism for this overshoot is related to the balance of forces in the boundary layer: for the low electrical conductivities near a cold wall the retarding magnetic force may not be able to overcome the accelerating effect of the favorable pressure gradient.

This issue was examined computationally in this work for the case $\sigma = (T/T_0)^4$. Here σ is the nondimensional conductivity and T_0 is the stagnation temperature. This formulation allows convenient comparison with the constant conductivity case ($\sigma = 1$ everywhere) because the conductivity between the shock and the boundary layer edge is $\sigma \approx 1$, since $T \approx T_0$.

Figure 12 shows the computed velocity profiles at $\theta = 6.6°$ (Fig. 12a) and the corresponding profiles predicted by the combined viscous and inviscid theories (Fig. 12b). Excellent agreement is seen between computation and theory in the shape of the boundary profiles. As discussed earlier, the inviscid theory tends to over-predict the edge velocity gradient, so there is some discrepancy between computation and theory in the values of the edge velocity. (Note that disagreement in the edge velocity was not present in Fig. 8 because the inviscid computations rather than the inviscid theory were used as input to the boundary layer theory calculations.) In both the computational and theoretical results, an overshoot in the velocity profile is seen to develop gradually as the interaction parameter is increased.

Bush's boundary layer theory also predicts, for the variable conductivity case, a diminished effectiveness of magnetic control in mitigating the stagnation point heat transfer. This trend was also observed computationally. For the constant conductivity case, the stagnation point heat transfer was reduced by 17% at $Q = 3$ and 28% at $Q = 6$; the corresponding results with variable conductivity were only 12% and 23%. A similar trend was seen for the shock standoff. The computed standoff increased over the non-magnetic case by 39% at $Q = 3$ and 83% at $Q = 6$; the corresponding results with variable conductivity were 24% and 56%.

Conclusions

Computational and theoretical studies of a hypersonic flow over a hemisphere were carried out to examine the possibility of heat transfer mitigation through magnetic control. The flow was studied in the low magnetic Reynolds number approximation, with an imposed dipole field. Both theory and numerical computations indicate that the applied field can slow the flow in the conductive shock layer and consequently reduce the wall heat flux in the vicinity of the stagnation point.

Excellent agreement was obtained between the viscous computations and boundary layer theory, whereas only fair agreement was found between the inviscid computations and the constant density theory. This discrepancy is consistent with the fact that the asymptotic constant density theory is accurate only for very high shock density ratios (Fig. 2), and tends to overpredict the stagnation point velocity gradient (Fig. 6). The combined theory predicts a somewhat higher level of heat transfer than that obtained computationally, but both theory and computation predict a similar change with increasing interaction parameter.

Nonuniform electrical conductivity was found, in

both theory and computation, to reduce the effectiveness of magnetic control. The significant effect of conductivity variations on the flow structure indicates the need in computations for an accurate electrical conductivity model in order to obtain good agreement with experimental data.

Magnetic control is seen to have a sound physical basis, and may prove to be a useful technology for heat transfer mitigation. In ongoing work, we are attempting to verify some of the other trends predicted in early theoretical studies (see the Introduction). Of particular interest are the effects of low Reynolds number, high magnetic Reynolds number, boundary layer separation, and the Hall current.

References

[1]Kantrowitz, A. R., "A Survey of Physical Phenomena Occurring in Flight at Extreme Speeds," *Proceedings of the Conference on High-Speed Aeronautics*, edited by A. Ferri, N. J. Hoff, and P. A. Libby, Polytechnic Institute of Brooklyn, New York, 1955, pp. 335–339.

[2]Bond, Jr., J. W., "Plasma Physics and Hypersonic Flight," *Jet Propulsion*, Vol. 28, No. 4, 1958, pp. 228–235.

[3]Resler, E. L. and Sears, W. R., "The Prospects for Magneto-Aerodynamics," *Journal of the Aeronautical Sciences*, Vol. 25, No. 4, 1958, pp. 235–245,258.

[4]Resler, E. L. and Sears, W. R., "The Prospects for Magneto-Aerodynamics – Correction and Addition," *Journal of the Aero/Space Sciences*, Vol. 26, No. 5, 1959, pp. 318.

[5]Sears, W. R., "Magnetohydrodynamic Effects in Aerodynamic Flows," *American Rocket Society Journal*, Vol. 29, No. 6, 1959, pp. 397–406.

[6]Donaldson, C. d. P. and Brunner, M. J., "Discussion of a Self-Powered MHD Control for Re-entry Vehicle Application," *Engineering Aspects of Magnetohydrodynamics: Proceedings, 3rd Symposium*, edited by N. W. Mather and G. W. Sutton, Gordon and Breach Science Publishers, New York, 1964, pp. 559–577.

[7]Kranc, S., Porter, R. W., and Cambel, A. B., "Electrodeless Magnetogasdynamic Power During Entry," *Journal of Spacecraft and Rockets*, Vol. 4, No. 6, 1967, pp. 813–815.

[8]Phillips, R. L., "Effect of Magnetic Drag on Re-Entry Body Heating," *American Rocket Society Journal*, Vol. 31, No. 5, 1961, pp. 672–674.

[9]Ericson, W. B. and Maciulaitis, A., "Investigation of Magnetohydrodynamic Flight Control," *Journal of Spacecraft and Rockets*, Vol. 1, No. 3, 1964, pp. 283–289.

[10]Boynton, J. H., "Experimental Study of an Ablating Sphere With Hydromagnetic Effect Included," *Journal of the Aero/Space Sciences*, Vol. 27, No. 4, 1960, pp. 306–307.

[11]Romig, M. F., "The Influence of Electric and Magnetic Fields on Heat Transfer to Electrically Conducting Fluids," *Advances in Heat Transfer*, edited by T. F. Irvine and J. P. Hartnett, Vol. 1, Academic Press, New York, 1964, pp. 267–354.

[12]Neuringer, J. L. and McIlroy, W., "Incompressible Two-Dimensional Stagnation-Point Flow of an Electrically Conducting Viscous Fluid in the Presence of a Magnetic Field," *Journal of the Aeronautical Sciences*, Vol. 25, No. 3, 1958, pp. 194–198.

[13]Neuringer, J. L. and McIlroy, W., "Hydromagnetic Effects on Stagnation-Point Heat Transfer," *Journal of the Aeronautical Sciences*, Vol. 25, No. 5, 1958, pp. 332–334.

[14]Rossow, V. J., "Magnetohydrodynamic Analysis of Heat Transfer Near a Stagnation Point," *Journal of the Aeronautical Sciences*, Vol. 25, No. 5, 1958, pp. 334–335.

[15]Meyer, R. C., "On Reducing Aerodynamic Heat-Transfer Rates by Magnetohydrodynamic Techniques," *Journal of the Aero/Space Sciences*, Vol. 25, No. 9, 1958, pp. 561–566,572.

[16]Meyer, R. X., "Magnetohydrodynamics and Aerodynamic Heating," *American Rocket Society Journal Journal*, Vol. 29, No. 3, 1959, pp. 187–192.

[17]Ziemer, R. W. and Bush, W. B., "Magnetic Field Effects on Bow Shock Stand-off Distance," *Physical Review Letters*, Vol. 1, No. 2, 1958, pp. 58–59.

[18]Bush, W. B., "Magnetohydrodynamic-Hypersonic Flow Past a Blunt Body," *Journal of the Aero/Space Sciences*, Vol. 25, No. 11, 1958, pp. 685–690,728.

[19]Kemp, N. H., "On Hypersonic Stagnation-Point Flow with a Magnetic Field," *Journal of the Aeronautical Sciences*, Vol. 25, No. 6, 1958, pp. 405–407.

[20]Bush, W. B., "A Note on the Magnetohydrodynamic-Hypersonic Flow Past a Blunt Body," *Journal of the Aero/Space Sciences*, Vol. 26, No. 8, 1959, pp. 536–537.

[21]Freeman, N. C., "On the Flow Past a Sphere at Hypersonic Speed With a Magnetic Field," *Journal of the Aero/Space Sciences*, Vol. 26, No. 10, 1959, pp. 670–672.

[22]Kemp, N. H., "Author's Reply," *Journal of the Aero/Space Sciences*, Vol. 26, No. 10, 1959, pp. 670–672.

[23]Hida, K., "An Approximate Study on the Detached Shock Wave in front of a Circular Cylinder and a Sphere," *Journal of the Physical Society of Japan*, Vol. 8, No. 6, 1953, pp. 740–745.

[24]Lykoudis, P. S., "The Matching of the Viscid and Inviscid Regions for the Stagnation Magnetic Flow," *Journal of the Aero/Space Sciences*, Vol. 26, No. 5, 1959, pp. 315–317.

[25]Kemp, N. H., "Hydromagnetic Effects on Heating and Shear at a Three-Dimensional Stagnation Point in Hypersonic Flow," *Journal of the Aero/Space Sciences*, Vol. 27, No. 7, 1960, pp. 553–554.

[26]Bush, W. B., "The Stagnation-Point Boundary Layer in the Presence of an Applied Magnetic Field," *Journal of the Aerospace Sciences*, Vol. 28, No. 8, 1961, pp. 610–611,630.

[27]Lykoudis, P. S., "Velocity Overshoots in Magnetic Boundary Layers," *Journal of the Aerospace Sciences*, Vol. 28, No. 11, November 1961, pp. 896–897.

[28]Andrade, C. A., "Magnetogasdynamic Shock Layer Flow," *Engineering Aspects of Magnetohydrodynamics: Proceedings, 2nd Symposium*, edited by C. Mannal and N. W. Mather, Columbia University Press, New York, 1962, pp. 107–120.

[29]Pai, S. I. and Kornowski, E. T., "Stagnation-Point Flow of a Magnetized Body in Hypersonic Flow," *Engineering Aspects of Magnetohydrodynamics: Proceedings, 2nd Symposium*, edited by C. Mannal and N. W. Mather, Columbia University Press, New York, 1962, pp. 97–106.

[30]Chushkin, P. I., "Magnetized Blunt Bodies in a Hypersonic Gas Flow," *Magnetohydrodynamics*, Vol. 1, No. 3, 1965, pp. 49–55, (*Magnitnaya Gidrodinamika*, Vol. 1, No. 3, 1965, pp. 67-75).

[31]Coakley, J. F. and Porter, R. W., "Time-Dependent Numerical Analysis of MHD Blunt Body Problem," *AIAA Journal*, Vol. 9, No. 8, 1971, pp. 1624–1626.

[32]Palmer, G., "Magnetic Field Effects on the Computed Flow over a Mars Return Aerobrake," *Journal of Thermophysics and Heat Transfer*, Vol. 7, No. 2, 1993, pp. 294–301.

[33]Ziemer, R. W., "Experimental Investigation in Magneto-Aerodynamics," *American Rocket Society Journal*, Vol. 29, No. 9, 1959, pp. 642–647.

[34]Seeman, G. R. and Cambel, A. B., "Observations Concerning Magnetoaerodynamic Drag and Shock Standoff Distance," *Proceedings of the National Academy of Sciences*, Vol. 55, No. 3, 1966, pp. 457–465.

[35]Nowak, R., Kranc, S., Porter, R. W., Yuen, M. C., and Cambel, A. B., "Magnetogasdynamic Re-Entry Phenomena," *Journal of Spacecraft and Rockets*, Vol. 4, No. 11, 1967, pp. 1538–1542.

[36]Kranc, S., Yuen, M. C., and Cambel, A. B., "Experimental Investigation of Magnetoaerodynamic Flow Around Blunt Bodies," NASA Contractor Report 1393, National Aeronautics and Space Administration, Washington, DC, August 1969.

[37]Wilkinson, J. B., "Magnetohydrodynamic Effects on Stagnation-Point Heat Transfer from Partially Ionized Nonequilibrium Gases in Supersonic Flow," *Engineering Aspects of Magnetohydrodynamics: Proceedings, 3rd Symposium*, edited by N. W. Mather and G. W. Sutton, Gordon and Breach Science Publishers, New York, 1964, pp. 413–438.

[38]Oguchi, H., "Blunt Body Viscous Layer with and without a Magnetic Field," *The Physics of Fluids*, Vol. 3, No. 4, 1960, pp. 567–580.

[39]Wu, C.-S., "Hypersonic Viscous Flow Near the Stagnation Point in the Presence of Magnetic Field," *Journal of the Aerospace Sciences*, Vol. 27, No. 12, 1960, pp. 882–893,950.

[40]Smith, M. C. and Wu, C.-S., "Magnetohydrodynamic Hypersonic Viscous Flow Past a Blunt Body," *AIAA Journal*, Vol. 2, No. 5, 1964, pp. 963–965.

[41]Smith, M. C., Schwimmer, H. S., and Wu, C.-S., "Magnetohydrodynamic-Hypersonic Viscous and Inviscid Flow Near the Stagnation Point of a Blunt Body," *AIAA Journal*, Vol. 3, No. 7, 1965, pp. 1365–1367.

[42]Porter, R. W. and Cambel, A. B., "Comment on 'Magnetohydrodynamic-Hypersonic Viscous and Inviscid Flow Near the Stagnation Point of a Blunt Body'," *AIAA Journal*, Vol. 4, No. 5, 1966, pp. 952–953.

[43]Smith, M. C., Schwimmer, H. S., and Wu, C.-S., "Reply by Authors to R. W. Porter and A. B. Cambel," *AIAA Journal*, Vol. 4, No. 5, 1966, pp. 953.

[44]Chen, S. Y., "Magnetic Hypersonic Flow near the Stagnation Point at Low Reynolds Number," *Journal of Spacecraft and Rockets*, Vol. 6, No. 8, 1969, pp. 872–877.

[45]Levy, R. H., "A Simple MHD Flow with Hall Effect," *AIAA Journal*, Vol. 1, No. 3, 1963, pp. 698–699.

[46]Porter, R. W. and Cambel, A. B., "Hall Effect in Flight Magnetogasdynamics," *AIAA Journal*, Vol. 5, No. 12, 1967, pp. 2208–2213.

[47]Porter, R. W. and Cambel, A. B., "Magnetic Coupling in Flight Magnetoaerodynamics," *AIAA Journal*, Vol. 5, No. 4, 1967, pp. 803–805.

[48]Anderson, D. A., Tannehill, J. C., and Pletcher, R. H., *Computational Fluid Mechanics and Heat Transfer*, Hemisphere Publishing, New York, 1st ed., 1984.

[49]Gaitonde, D. V., "Development of a Solver for 3-D Non-Ideal Magnetogasdynamics," AIAA Paper 99-3610, June 1999.

[50]Jameson, A., Schmidt, W., and Turkel, E., "Numerical Solutions of the Euler Equations by a Finite Volume Method Using Runge-Kutta Time Stepping Schemes," AIAA Paper 81-1259, 1981.

[51]Conte, S. and de Boor, C., *Elementary Numerical Analysis: An Algorithmic Approach*, McGraw-Hill, New York, 1980.

[52]de Hoffmann, F. and Teller, E., "Magneto-Hydrodynamic Shocks," *Physical Review*, Vol. 80, No. 4, 1950, pp. 692–703.

[53]Ambrosio, A. and Wortman, A., "Stagnation Point Shock Detachment Distance for Flow Around Spheres and Cylinders," *ARS Journal*, Vol. 32, No. 2, 1962, pp. 281.

[54]Fay, J. A. and Riddell, F. R., "Theory of Stagnation Point Heat Transfer in Dissociated Air," *Journal of the Aeronautical Sciences*, Vol. 25, No. 2, 1958, pp. 73–85,121.

[55]White, F. M., *Viscous Fluid Flow*, McGraw-Hill, New York, 1st ed., 1974.

[56]Anderson, J. D., *Hypersonic and High Temperature Gas Dynamics*, McGraw-Hill, New York, 1989.